CHAPTER TWENTY-FIVE

Supply–Demand Analysis: A Framework for Exploring the Regulatory Design of Metabolism

Jan-Hendrik S. Hofmeyr*,† *and* Johann M. Rohwer*

Contents

Abstract

The living cell can be thought of as a collection of linked chemical factories, a molecular economy in which the principles of supply and demand obtain. Supply–demand analysis is a framework for exploring and gaining an understanding of metabolic regulation, both theoretically and experimentally, where regulatory performance is measured in terms of flux control and homeostatic maintenance of metabolite concentrations. It is based on a metabolic control analysis of a supply–demand system in steady state in which the degree of flux and concentration control by the supply and demand blocks is related to their local properties, which are quantified as the elasticities of supply and demand. These elasticities can be visualized as the slopes of the log–log rate characteristics of supply and demand. Rate characteristics not only provide insight about

* Department of Biochemistry, University of Stellenbosch, Private Bag X1, Stellenbosch, South Africa
† Centre for Studies in Complexity, University of Stellenbosch, Private Bag X1, Stellenbosch, South Africa

Methods in Enzymology, Volume 500
ISSN 0076-6879, DOI: 10.1016/B978-0-12-385118-5.00025-6

system behavior around the steady state but can also be expanded to provide a view of the behavior of the system over a wide range of concentrations of the metabolic intermediate that links the supply and the demand. The theoretical and experimental results of supply–demand analysis paint a picture of the regulatory design of metabolic systems that differs radically from what can be called the classical view of metabolic regulation, which generally explains the role of regulatory mechanisms only in terms of the supply, completely ignoring the demand. Supply–demand analysis has recently been generalized into a computational tool that can be used to study the regulatory behavior of kinetic models of metabolic systems up to genome-scale.

1. Introduction

Supply–demand analysis (Hofmeyr, 2008; Hofmeyr and Cornish-Bowden, 2000) is a framework for exploring and gaining an understanding of metabolic regulation, both theoretically and experimentally, and is the culmination of a series of studies initiated in the early 1990s (Hofmeyr, 1995; Hofmeyr and Cornish-Bowden, 1991, 1996; Hofmeyr *et al.*, 1993). Rohwer and Hofmeyr (2008) recently generalized supply–demand analysis into a computational tool for analyzing regulation in kinetic models of cellular systems of any complexity.

The concept of metabolic regulation is tightly linked to metabolic function, such as, for example, the control of flux, the homeostatic maintenance of metabolite concentrations, the control of transition time between steady states, or the dynamic and structural stability of the steady state. Therefore, to say that a system is regulated is to mean that its intrinsic properties have been molded by evolution to fulfill specific functions (Hofmeyr, 1995; Hofmeyr and Cornish-Bowden, 1991). Because mass action is the intrinsic driving force for self-organization of reaction networks, we broadly define metabolic regulation as *the alteration of reaction properties to augment or counteract the mass-action trend in a network of reactions* (Hofmeyr, 1995; Reich and Sel'kov, 1981; Rohwer and Hofmeyr, 2010). In supply–demand analysis, we measure regulatory performance in terms of flux control and homeostatic maintenance of metabolite concentrations.

Whereas the classical view of metabolic regulation usually considers the biosynthetic pathway in isolation without considering what happens to the products—a situation that we have likened to an economic analysis of a factory that ignores the consumption of the products of the factory (Hofmeyr and Cornish-Bowden, 2000)—supply–demand analysis takes the demand into consideration. What results from this has led Oliver (2002) to remark that it "could mean that biologists in the twenty-first century need a rethink of their view of cellular economy that is every bit as

radical as that initiated for political economy by John Stuart Mill and William Stanley Jevons in the nineteenth century."

One of the most powerful features of supply–demand analysis is a tool, the graph of combined rate characteristics, with which to visualize the regulatory design of a metabolic system. In the complex system of interacting processes that is the living cell, the properties of the agents that facilitate these processes, such as enzymes, transporters, and receptors, must be tuned to each other if the system is to behave harmoniously. To our knowledge, the graph of combined rate characteristics is the only way of visually combining all these properties in one picture.

2. The Functional Organization of Metabolism

The living cell can be thought of as a collection of linked chemical factories, a molecular economy in which the principles of supply and demand obtain. Biochemical textbooks and the ubiquitous wall charts depicting metabolic pathways tend to obscure this functional organization of the metabolism of all living organisms into blocks that produce and consume metabolic products (Fig. 25.1). These metabolic blocks communicate with each other through intermediates that couple the blocks by either the linear or the cyclic linkage types depicted in Fig. 25.2.

In the cyclic system, the sum of the concentrations of X and Y is constant; they form a moiety-conserving cycle (Hofmeyr *et al.*, 1986). X and Y can therefore vary only within this constraint, which, in turn, implies that the cycle can be reduced to a linear system with the concentration ratio y/x (or its inverse) as the coupling variable. If, for example, Y is ATP and X is ADP, ATP can be regarded as the phosphate-charged form of the ADP moiety, so that y/x is the ratio of charged over uncharged moiety. Hofmeyr (1997) has shown that even in more complex cycles, such as the ATP–ADP–AMP system in the presence of an active adenylate kinase, this principle still holds: here, the charged over uncharged ratio is $([ATP] + 0.5[ADP])/([AMP] + 0.5[ADP])$.

3. Quantitative Analysis of Supply–Demand Systems

The question as to how the properties of the supply and demand blocks determine the behavior and control of the steady-state flux and concentration of the intermediate (p or y/x in Fig. 25.2) can be answered within the framework of metabolic control analysis (Heinrich and Rapoport, 1974; Kacser *et al.*, 1995). Here, we use combined log–log rate characteristics (Hofmeyr, 1995) as a powerful visual aid to explain the analysis.

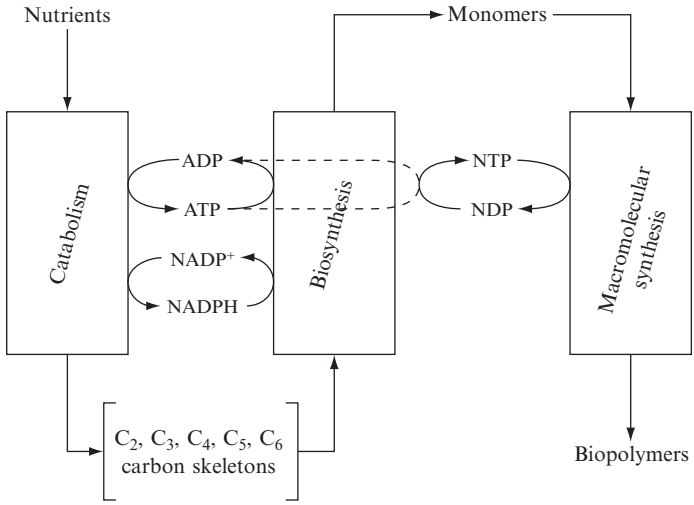

Figure 25.1 The functional organization of intermediary metabolism. The primary energy sources are degraded by catabolic pathways to form ATP, reducing equivalents (NADPH), and C_3—C_6 metabolic intermediates (e.g., sugar phosphates, activated CoA intermediates, PEP, pyruvate, oxaloacetate, and 2-oxoglutarate) that act as carbon skeletons for biosynthetic (anabolic) processes that produce monomers for the synthesis of biopolymers (proteins from amino acids, nucleic acids from nucleotides, lipids from fatty acids) and higher-order cellular structures; these processes also require an input of free energy (NTP, nucleotide triphosphates).

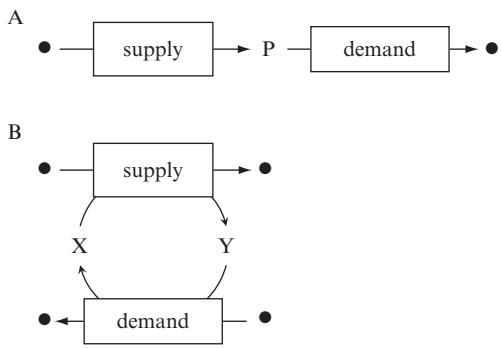

Figure 25.2 Two ways in which metabolic supply and demand reaction blocks are linked. (A) linear; (B) cyclic. In the linear system, the demand takes the linking metabolite P on to form a further product (here depicted by a solid circle). In the cyclic system, the demand reverses the action of the supply as far as the linking metabolite is concerned. For example, if the supply oxidizes X, the demand reduces it, or if the supply phosphorylates X to form Y, the demand dephosphorylates Y back to X.

Figure 25.3 shows how the steady state of a supply–demand system is formed and how the distribution of flux and concentration control depends on the properties of the supply and demand blocks. On the graph, the natural logarithms of the supply and demand rates are plotted as a function of the natural logarithm of the concentration variable that links them. If the supply and demand were catalyzed by single enzymes, these curves would represent, for example, the familiar Michaelis–Menten or Hill responses of a rate with respect to a product or a substrate. In general, however, the supply and demand are reaction blocks, so that the rate curves actually represent the variation in the local steady-state fluxes of the isolated supply and demand blocks as they respond to variation in the concentration of P. The use of logarithmic rather than linear scales has a number of advantages (Hofmeyr, 1995), the most important being that it allows direct comparison of the magnitude of steady-state responses to perturbations at different positions of the rate and concentration scale (equal distances on different parts of a logarithmic axis represent equal percentage change in the variable represented on that axis). Another advantage is that the curves retain their form when they vary with a parameter that is a multiplier of the rate equation, such as enzyme concentration.

The intersection of the supply and demand rate characteristic represents the steady state, which is characterized by a flux, J, and concentration of P, $\bar{p}$. From the graph, it should be clear that the response in the steady state to small perturbations in the activities of supply or demand depends completely on the *elasticity coefficients*, that is, the slopes of the tangents to the double logarithmic rate characteristics at the steady-state point.

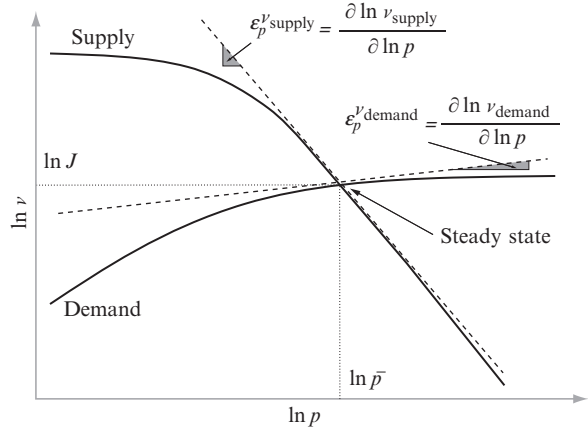

Figure 25.3 The rate characteristics of a supply–demand system plotted in double logarithmic space, showing the steady state where the two rate characteristics intersect; J is the steady-state flux, and $\bar{p}$ is the steady-state concentration of P. The slopes of the tangents to the rate characteristics at the steady-state point are the so-called elasticities of the supply and demand rates with respect to P (Hofmeyr and Cornish-Bowden, 2000). Reproduced with permission from Hofmeyr and Cornish-Bowden (2000).

The control of the supply and demand blocks over the flux and concentration of P is quantified in terms of the response of these steady-state variables to small perturbations, $d \ln v_{\text{supply}}$ or $d \ln v_{\text{demand}}$ in the activities of the supply or demand blocks. The degrees to which supply and demand control J and $\bar{p}$ are given by the *flux–control coefficients*:

$$C^J_{\text{supply}} = \frac{d \ln J}{d \ln v_{\text{supply}}}; \quad C^J_{\text{demand}} = \frac{d \ln J}{d \ln v_{\text{demand}}} \tag{25.1}$$

and the *concentration-control coefficients*

$$C^p_{\text{supply}} = \frac{d \ln p}{d \ln v_{\text{supply}}}; \quad C^p_{\text{demand}} = \frac{-d \ln p}{d \ln v_{\text{demand}}} \tag{25.2}$$

Hofmeyr and Cornish-Bowden (2000) provide a graphical thought experiment that illustrates these definitions.

Flux-control and concentration-control coefficients obey the following summation relationships:

$$C^J_{\text{supply}} + C^J_{\text{demand}} = 1 \tag{25.3}$$

$$C^p_{\text{supply}} + C^p_{\text{demand}} = 0 \tag{25.4}$$

These are specific cases of the so-called *summation theorems* of control analysis (Kacser *et al.*, 1995).

Further, using the definitions of the elasticities of supply and demand given in Fig. 25.3, the *connectivity theorems* (Kacser *et al.*, 1995) can also be derived:

$$C^J_{\text{supply}} \varepsilon_p^{v_{\text{supply}}} + C^J_{\text{demand}} \varepsilon_p^{v_{\text{demand}}} = 0 \tag{25.5}$$

$$C^p_{\text{supply}} \varepsilon_p^{v_{\text{supply}}} + C^p_{\text{demand}} \varepsilon_p^{v_{\text{demand}}} = -1 \tag{25.6}$$

The summation and connectivity theorems provide enough information to express the control coefficients in terms of elasticities of supply and demand (Hofmeyr and Cornish-Bowden, 1991). The flux-control coefficients are

$$C^J_{\text{supply}} = \frac{\varepsilon_p^{v_{\text{demand}}}}{\varepsilon_p^{v_{\text{demand}}} - \varepsilon_p^{v_{\text{supply}}}} \tag{25.7}$$

and

$$C^{J}_{\text{demand}} = \frac{-\varepsilon_p^{\nu_{\text{supply}}}}{\varepsilon_p^{\nu_{\text{demand}}} - \varepsilon_p^{\nu_{\text{supply}}}} \tag{25.8}$$

and the concentration-control coefficients:

$$C^{p}_{\text{supply}} = -C^{p}_{\text{demand}} = \frac{1}{\varepsilon_p^{\nu_{\text{demand}}} - \varepsilon_p^{\nu_{\text{supply}}}} \tag{25.9}$$

Note that $\varepsilon_p^{\nu_{\text{supply}}}$ is typically a negative quantity, that is, product inhibits supply through enzyme inhibition and thermodynamic back-pressure. The ratio of elasticities determines the distribution of flux-control between supply and demand (if $\left|\varepsilon_p^{\nu_{\text{supply}}}/\varepsilon_p^{\nu_{\text{demand}}}\right| > 1$, the demand has more control over the flux than the supply; if $\left|\varepsilon_p^{\nu_{\text{supply}}}/\varepsilon_p^{\nu_{\text{demand}}}\right| < 1$, the demand has less control over the flux than the supply). With regard to $\bar{p}$, it is not the distribution of $\bar{p}$-control that is of interest (C^{p}_{supply} always being equal to $-\,C^{p}_{\text{demand}}$ no matter what the values of the elasticities), but what determines the magnitude of the variation in $\bar{p}$ (and, therefore, its homeostatic maintenance): the larger $\varepsilon_p^{\nu_{\text{demand}}} - \varepsilon_p^{\nu_{\text{supply}}}$, the smaller the absolute values of both C^{p}_{supply} and C^{p}_{demand}, and the better the homeostatic regulation of $\bar{p}$. This algebraic analysis is clearly illustrated by the different configuration of rate characteristics around the steady state shown in Fig. 25.4.

Figure 25.4A shows a situation where the absolute values of the elasticities of supply and demand (the slopes of the lines) are equal, so that the functions of flux and concentration control are equally distributed: the same percentage change in the activity of either supply or demand causes the same change in the flux ($C^{J}_{\text{supply}} = C^{J}_{\text{demand}} = 0.5$). The magnitude of the variation in $\bar{p}$ is determined to the same degree by the supply and demand elasticities. We call this a *functionally undifferentiated system*. Similarly, Fig. 25.4B shows a functionally undifferentiated system in which the elasticities of supply and demand are much smaller (shallower slopes). This clearly illustrates the principle that the sum of supply and demand elasticities determines the degree of concentration control of $\bar{p}$: the larger the sum, the smaller the values of the control coefficients.

In Fig. 25.4C and D, the elasticity of demand is decreased considerably (the demand becomes more saturated with P). Comparing equal percentage changes in demand (in C) and supply (in D), it is clear that most of the flux control has been transferred to the demand. However, because $\varepsilon_p^{\nu_{\text{demand}}} \ll \left|\varepsilon_p^{\nu_{\text{supply}}}\right|$, the magnitude of the variation in $\bar{p}$ is now largely determined by the supply elasticity. This phenomenon is even more pronounced in Fig. 25.4E and F where the supply slope is very steep. Therefore, the steeper the slope of the supply rate characteristic, the narrower the band of variation in $\bar{p}$ and, therefore, the better the homeostatic maintenance of $\bar{p}$. The opposite would

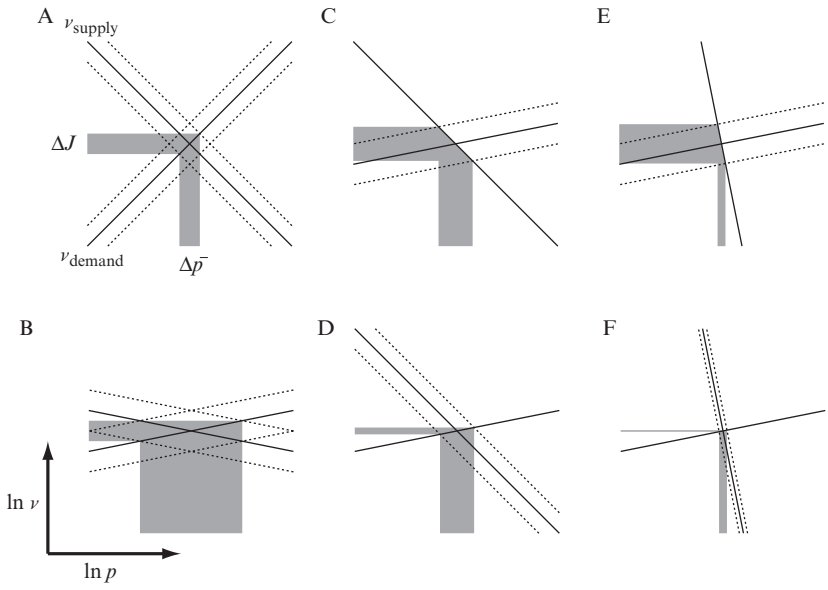

Figure 25.4 The effect on the steady state of varying the activity of the demand (C, E) or supply (D, F) or both (A, B). The slope of each line is an elasticity of either supply or demand at the steady state. The dotted lines show a set percentage increase or decrease in activity. The shaded regions show the magnitude of the response in the steady-state flux (horizontal) and concentration of P (vertical). See text for explanation.

obtain if the supply elasticity were small, whereas the demand elasticity were large: flux control would shift to the supply, while the elasticity of demand would determine the magnitude of variation in $\bar{p}$.

Supply–demand analysis therefore shows that the functions of flux and concentration control are mutually exclusive in the sense that if one block controls the flux, it loses any influence over the magnitude of variation in the concentration of the linking intermediate $\bar{p}$: this becomes the sole function of the other block. This finding has profound consequences for any view of metabolic regulation.

The above analysis has only considered the response of the steady state to small variations in the activity of supply or demand without considering either the form of the full rate characteristics or the position of the steady state in relation to equilibrium. Rate characteristics can also be used to obtain an overall view of the limits within which the system can fulfill its functions.

A supply pathway must be able to meet increasing demand for its product at least up to some limit and to cope with low demand in such a way that its product and intermediate metabolite concentrations do not tend toward their equilibrium concentrations (most biosynthetic pathways have huge equilibrium constants so that near-equilibrium conditions would cause

fatally high accumulation of supply pathway intermediates and product (Atkinson, 1977). Textbook wisdom has it that allosteric feedback inhibition of supply by its product is responsible for satisfying demand, while it has little to say about low demand. Supply–demand analysis teaches us otherwise.

Figure 25.5 shows a set of supply–demand rate characteristics that span the full range of p to its equilibrium value (assuming that the substrate for the supply pathway is buffered and therefore constant). For the supply to be able to meet a specific range of variation in demand activity, it cannot have any flux control in that range. Focusing for the moment on the supply curve, it is clear that only in the shaded band between steady states 2 and 3 will the supply be able to meet the variation in demand while keeping $\bar{p}$ reasonably constant. When demand becomes higher than 2, it loses control over the flux (steady state 1) with a concomitant sharp decrease in $\bar{p}$. An increase in the maximal activity of the supply (the plateau at 1) would extend the range in which the supply can meet the demand. However, it is also clear that the presence of allosteric feedback inhibition is not a prerequisite for flux control by demand: in the shaded band on the right, demand also controls the flux in the absence of allosteric feedback (the dashed supply characteristic), and the supply is equally effective in keeping $\bar{p}$ homeostatic. The dramatic difference between the two situations is in the concentration where P is homeostatically maintained: without feedback inhibition, it can only be near equilibrium (with all the accompanying disadvantages),

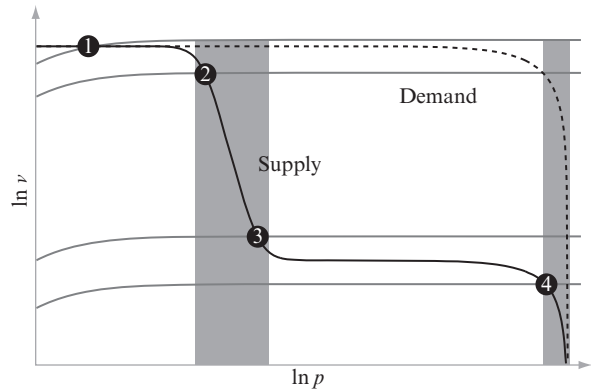

Figure 25.5 The steady-state behavior of a supply–demand system with (solid) and without (dashed) inhibition of supply by its product P. The gray lines represent different demand activities. The four marked steady states are discussed in the text. The rate characteristics were generated with PySCeS (Olivier *et al.*, 2005) for the supply–demand system described in Hofmeyr and Cornish-Bowden (1991) using the reversible Hill (Hofmeyr and Cornish-Bowden, 1997) and reversible Michaelis–Menten rate equations with realistic parameter values. Reproduced with permission from Hofmeyr and Cornish-Bowden (2000).

whereas with feedback inhibition, it can be maintained orders of magnitude away from equilibrium (at a concentration around the $p_{0.5}$ of the allosteric enzyme). Clearly, therefore, when demand controls flux, the functional role of feedback inhibition is homeostatic maintenance of $\bar{p}$ at a concentration far from equilibrium.

In general, each elasticity coefficient is the sum of a mass-action term that depends only on Γ/K_{eq} and a binding term that is determined by the binding properties of the enzyme. The mass-action term in the supply elasticity approaches 0 in conditions far from equilibrium and $-\infty$ near equilibrium, where it completely swamps the binding term, which typically varies between 0 and the Hill coefficient (Hofmeyr, 1995; Rohwer and Hofmeyr, 2010). Kinetic effects such as allosteric feedback inhibition can therefore only play a regulatory role far from equilibrium where the mass-action term is negligible. This is also shown by the solid curve in Fig. 25.5: there is a lower limit (around 3) to the range in which $\bar{p}$ can be kinetically regulated; below this limit, $\bar{p}$ jumps to the region where the mass-action term dominates the supply elasticity.

Hofmeyr (2008) considered a more complex version of the simple supply–demand system in Fig. 25.5, to which was added a catabolic demand for P and the induction of the synthesis of the first supply enzyme at low concentrations of P, with P acting as a corepressor. This allowed, on the one hand, for an increase in supply capacity at low P, thereby extending the range in which the supply could match variation in demand activity. However, the inclusion of a catabolic demand provided an overflow valve into which P could be channeled once the demand fell too low, thus preventing P to jump to near-equilibrium concentrations. However, for the system to function in this way, the parameters of all the various regulatory mechanisms had been carefully matched. First, the strength of binding of P to the repressor protein had to be matched to the strength of allosteric binding of P to the first supply enzyme in order to ensure a smooth transition in the supply rate characteristic from the regime of allosteric regulation to that of enzyme expression. Second, the binding properties of the catabolic demand had to be chosen so that it did not kick in at too low or too high a concentration of P; positive cooperative binding of P to the catabolic demand also increased the regulatory effectivity. This analysis showed in a particularly clear way the power of combined rate characteristics to visualize and understand the regulation design of metabolism in the way that, to our knowledge, no other method provides.

4. Generalized Supply–Demand Analysis

Ordinary supply–demand analysis of a kinetic model can be easily achieved *in silico* by making the intermediate around which the rate characteristic is to be constructed a fixed (clamped) species of the model, thus

turning it into a model parameter. This parameter is then varied over a wide range through a parameter scan. An implicit assumption of this approach is that the system has been or can readily be partitioned into supply and demand; however, when faced with the complexity of cellular pathways or of large models of such pathways, the choice of intermediate around which to perform the supply–demand analysis is often far from obvious. This has hampered the application of supply–demand analysis to large kinetic models of cellular pathways.

To address this shortcoming, we have generalized supply–demand analysis in such a way that it can easily be performed on a kinetic models of any cellular system, large or small, without requiring prior knowledge of its regulatory structure (Rohwer and Hofmeyr, 2008). Generalized supply–demand analysis works in the following way: *each* of the variable intermediates is *clamped in turn* and thus made into a parameter of the system. Its concentration is then varied above and below the reference steady-state value in the original system through a parameter scan, and the fluxes through the supply and demand reactions that are directly connected to the intermediate are plotted on a log–log rate characteristic. Every flux that directly produces the intermediate is a separate supply flux, and likewise, each flux that directly consumes it is a separate demand flux. There will thus be as many rate characteristics as there are reactions that produce or consume the intermediate. It should be emphasized that this procedure is valid for arbitrary models and does not presuppose a subdivision of the system into supply and demand blocks.

Generalized supply–demand analysis yields as many combined rate characteristic graphs as there are variable species in the system. As will be shown below, the following important features about the regulation of the system can be identified from the shapes of the curves and associated elasticities and response coefficients:

1. Potential sites of regulation;
2. Regulatory metabolites;
3. The quantitative relative contribution of different routes of interaction from an intermediate to a supply or demand block;
4. Sites of functional differentiation where one of the supply or demand blocks predominantly controls the flux, and the other determines the degree of homeostatic buffering of the intermediate.

We exemplify generalized supply–demand analysis with a model of a linear five-enzyme pathway containing a feedback loop. The simulations use two variants of a kinetic model of the linear pathway in Fig. 25.6; detailed model descriptions and computational methods are provided in Rohwer and Hofmeyr (2008).

Model I This is the base-line, undifferentiated version in which all five enzymes have identical kinetic parameters and are modeled with reversible

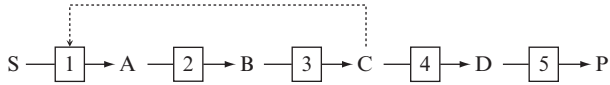

Figure 25.6 A five-enzyme linear pathway converting substrate S to product P. In one of the models, the first enzyme is allosterically inhibited by intermediate C (see main text). Reproduced with permission from Rohwer and Hofmeyr (2008).

Michaelis–Menten kinetics (with the exception of enzyme 5, which is modeled with irreversible Michaelis–Menten kinetics). There is no allosteric feedback from C to enzyme 1.

Model II In this model, enzyme 1 is inhibited allosterically by C and is modeled with reversible Hill kinetics (Hofmeyr and Cornish-Bowden, 1997). The limiting rates of enzymes 2 and 3 have been increased so that they are close to equilibrium. Enzymes 4 and 5 together have almost complete control over the flux through the pathway.

As explained above, a generalized supply–demand analysis is performed by clamping each variable species of the model, in turn, and varying its concentration to generate the supply and demand rate characteristics. This yields graphs such as in Fig. 25.7, which shows the generalized supply–demand analysis around metabolite B in model I. To facilitate the interpretation of such graphs, this specific case is discussed in detail. The intersection of the log–log rate characteristics of supply and demand marks the steady-state point. The supply rate characteristic is drawn in light gray and the demand rate characteristic in medium gray. The slopes of the tangents to the rate characteristics (indicated by dashed lines on the graph) equal the flux–response coefficients (see e.g., Kacser *et al.*, 1995) of supply and demand toward B (in Fig. 25.7, J_{12} signifies the flux through the supply block and J_{345} that through the demand block). These response coefficients quantify how sensitively the supply and demand fluxes respond toward changes in b and are equivalent to "block-elasticities" (Fell and Sauro, 1985) or coresponse coefficients (Hofmeyr and Cornish-Bowden, 1996; Hofmeyr *et al.*, 1993) in the complete system where B is not clamped.

Supply–demand analysis as described in Section 3 assumes that the only communication between supply and demand is via the linking intermediate. In this situation, the supply–demand block control coefficients of the complete pathway can be directly calculated from the supply and demand block elasticities (see Eqs. (25.7)–(25.9)), and the distribution of flux control is determined by the ratio of the block elasticities, while the magnitude of concentration control is determined by the difference $\varepsilon_b^{\nu_{345}} - \varepsilon_b^{\nu_{12}}$. Figure 25.7 also shows graphically the elasticities of the enzymes that produce or consume B. In this case, B is a product of ν_2 and a substrate for ν_3, so Fig. 25.7 shows $\varepsilon_b^{\nu_2}$ (thick light gray line) and $\varepsilon_b^{\nu_3}$ (thick medium gray line).

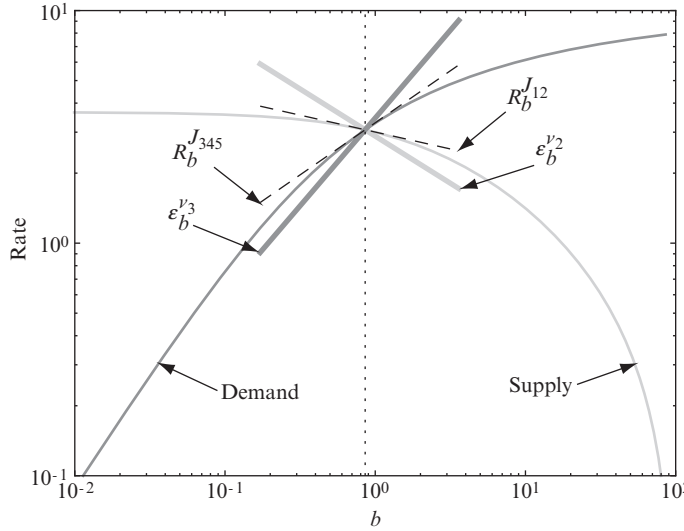

Figure 25.7 Supply–demand analysis around metabolite *B* for Model I. The concentration of *B* was clamped and varied to generate the supply and demand rate characteristics, as described in the text. The steady-state concentration is indicated by a vertical dotted line. The rate characteristics, response coefficients (tangents to the rate characteristics at the steady-state point), and elasticities of the supply and demand enzymes directly connected to *B* are labeled on the graph. Reproduced with permission from Rohwer and Hofmeyr (2008).

The crux of generalized supply–demand analysis now lies in the comparison of the values of the response coefficients with the elasticities of the enzymes that are directly connected to the clamped metabolite. In Fig. 25.7, these values differ, that is, $R_b^{J12} \neq \varepsilon_b^{v2}$ and $R_b^{J345} \neq \varepsilon_b^{v3}$. In other cases, they will be seen to agree. However, before comparing them in detail, first we have to present the generalized supply–demand analysis of all metabolites for both models.

The graphs in Fig. 25.8 present the results of the generalized supply–demand analysis on models I and II. To avoid clutter, the graphs are not annotated but they follow the same convention as Fig. 25.7. The only additional piece of information required is that of an allosteric modifier elasticity (ε_c^{v1} in Fig. 25.8B with *c* clamped, as only model II has the feedback loop). This is drawn in a dark gray line to set it apart from the supply and demand elasticities.

For larger models where a particular metabolite may be connected to a number of different supply and demand fluxes and the overall graph is too cluttered, the individual rate characteristics for each flux and their associated elasticity and response coefficients can be drawn on separate graphs. This choice depends on the particular model analyzed, but ultimately, it is only a

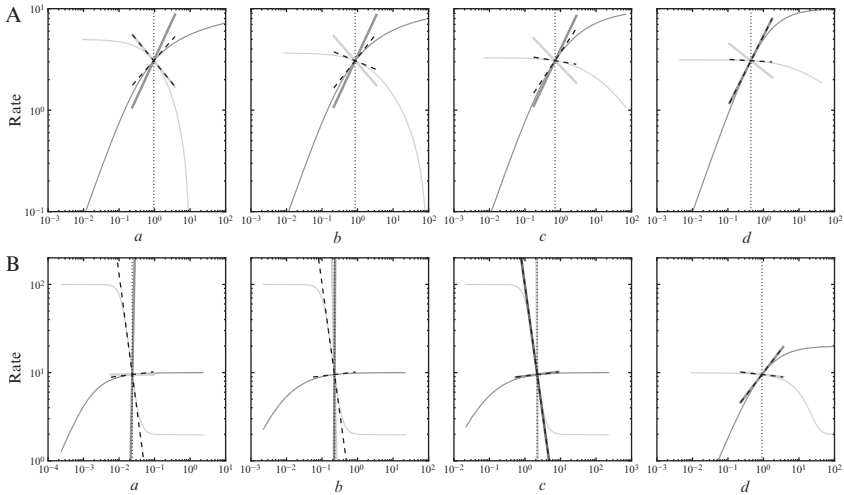

Figure 25.8 Generalized supply–demand analysis of the system depicted in Fig. 25.6. The concentrations *a–d* were clamped, in turn, and varied to generate the supply and demand rate characteristics, as described in the text. The supply rate characteristic is drawn in light gray, that for the demand in medium gray. The steady-state concentration of the clamped metabolite is indicated by a vertical dotted line. The response coefficients of the supply and demand blocks are indicated by black dashed lines. The elasticities of the supply and demand enzymes for the clamped intermediate they are directly connected to are indicated by thick lines of the same color as the rate characteristic. Model variants: (A) model I, (B) model II (see main text). In (B), the allosteric elasticity $\varepsilon_c^{v_1}$ is indicated by a dark gray thick line. Adapted from Rohwer and Hofmeyr (2008) with permission.

question of visualizing the data and in no way changes the principle of the analysis.

The graphs in Fig. 25.8 contain a wealth of information. As shown in Rohwer and Hofmeyr (2008), they can be interpreted on four levels, that is, differences in the rate characteristic shapes as one proceeds from one metabolite to the next in the pathway, comparison of elasticity and response slopes, identification of points of functional differentiation and homeostasis, and finally, refined analysis through partial response coefficients.

4.1. Differences in rate characteristic shapes

The first assessment criterion of generalized supply–demand analysis merely looks at the general shapes of the supply and demand rate characteristics and is not yet concerned with elasticities and response coefficients. In model I (Fig. 25.8A), all enzymes have identical kinetics and the overall shapes of the rate characteristics are similar for metabolites *A–D*. In model II (Fig. 25.8B),

however, the pattern for D is different from those for A–C (which are still similar). This means that the kinetic properties of enzyme 4 are such that site of regulation has been introduced into the system. In this specific case, the reason is that enzyme 4 has been made insensitive to changes in the concentration of C ($\varepsilon_c^{v_4} \approx 0$). In general, such zero elasticities, whether toward substrate or product, induce a change in the rate characteristic shape because they shift the flux control to demand or supply, respectively. Overall, changes in the rate characteristic shapes thus pin-point potential sites of regulation.

4.2. Comparison of elasticities and response coefficients

Generalized supply–demand analysis can be extended to a second level by comparing the values of the elasticities and flux–response coefficients at the steady-state point for each metabolite. From the partitioned response property of control analysis (Kacser *et al.*, 1995),

$$R_p^J = \varepsilon_p^{v_i} \times C_{v_i}^J \tag{25.10}$$

it follows that $R_p^J = \varepsilon_p^{v_i}$ if $C_{v_i}^J = 1$. This means that the enzyme on which the intermediate acts directly must have full control over its own flux. Figure 25.8 shows that in general, response and elasticity coefficients differ. There are, however, a few notable exceptions. The first of these is the trivial case of the first and last metabolites in the chain (A and D): response coefficients and elasticities will generally agree because the supply block for A and demand block for D each consists only of a single enzyme. (The exception of $\varepsilon_a^{v_1} \neq R_a^{J_1}$ in Fig. 25.8B has to do with the feedback loop and is further discussed in Rohwer and Hofmeyr (2008).)

Aside from the trivial case, any agreement between elasticity and response coefficient points to a site of regulation. Eq. (25.10) shows that the response coefficient can equal the elasticity either if the control coefficient is one (as discussed above), or if the elasticity is zero (which effectively makes the value of the control coefficient irrelevant). The first case obtains, for example, in Fig. 25.8B with c clamped, where $\varepsilon_c^{v_1} = R_c^{J_{123}}$ (feedback loop with $C_{v_1}^{J_{123}} = 1$). Here, C can be classified as a "regulatory metabolite" with respect to its supply block because the flux response of this supply toward the clamped metabolite concentration is exactly the same as the activity response (i.e., elasticity) of the enzyme directly affected by the clamped metabolite. The flux-control coefficient of one causes the flux response to be transmitted fully through the block.

The second case (zero elasticity) obtains, for example, in Fig. 25.8B, where $\varepsilon_c^{v_4} = R_c^{J_{45}} \approx 0$. Such a zero elasticity confers flux control (in the complete system) to that particular block and results in functional differentiation of the system, which is further discussed below.

4.3. Functional differentiation and homeostasis

Functional differentiation has been discussed in Section 3 (see also Fig. 25.4) and is characterized by flux- and concentration control being functions of different blocks. Complete flux control by a supply or demand block (over the whole pathway) can easily be identified by a zero response coefficient (i.e., block elasticity) of that block toward the intermediate (e.g., R_c^{J45} in Fig. 25.8B). The response coefficient of the other block (R_c^{J123}) will then determine the degree of homeostasis in the intermediate: the larger its numerical value, the better the homeostatic buffering. In model II (Fig. 25.8B), the properties of the feedback elasticity $\varepsilon_c^{v_1}$, which equals R_c^{J123} here, set the steady-state concentration of C and determine its degree of homeostatic buffering. In this sense, the steady-state concentration of C can be regarded as "regulated." Why C can be considered a "regulatory" metabolite when considering the supply block in isolation has been discussed above.

4.4. Multiple routes of interaction

When two or more direct routes of interaction exist from a clamped metabolite to a particular supply or demand block, generalized supply–demand analysis can be further refined by dissecting the response coefficient into partial response coefficients. An example is the generalized supply–demand analysis around metabolite C in Fig. 25.6, where C can affect both enzymes 1 and 3 directly (the former through allosteric inhibition, the latter through product inhibition). By calculating the total response coefficient as the sum of the two partial response coefficients referring to each of these routes of interaction, their individual contribution to the total response coefficient can be quantified and depicted graphically. This will not be further discussed here, and the reader is referred to Rohwer and Hofmeyr (2008).

4.5. Requirements for and limitations of the approach

Generalized supply–demand analysis, by virtue of being a computational method, requires a fully parameterized kinetic model. This is of course a limitation because such models do not exist for all pathways; however, their number and size are increasing steadily as any regular inspection of the JWS Online (Olivier and Snoep, 2004) or BioModels (le Novère *et al.*, 2006) databases will show. The application of the approach is thus limited by the size of available models, but this is not a limitation of the analysis *per se*. Indeed, efforts are under way toward building a genome-scale model of cellular metabolism (Smallbone *et al.*, 2010), and there is no reason in principle why generalized supply–demand analysis cannot be applied to such a model.

It could be argued naively that if a kinetic model of a pathway is available, then we know all the relevant regulatory mechanisms, so why is generalized supply–demand analysis necessary and what new insight can we gain from it? However, by way of example, the mere presence of a feedback loop does not mean that it is always active, and under some conditions, (such as very high demand in the pathway discussed by Hofmeyr and Cornish-Bowden, 2000) the regulation may actually follow a different route. Generalized supply–demand analysis thus identifies active routes of regulation under a *particular set of conditions*; these are dynamic properties of the model and depend on its particular state, they cannot be inferred from model structure alone. In addition, as the size of kinetic models increases (Smallbone *et al.*, 2010), their level of complexity approaches that of the systems they model. Tools are thus required for interrogating and analyzing such models, and generalized supply–demand analysis provides a first point of entry for such an analysis.

5. Experimental Applications of Supply–Demand Analysis

This section deals with methods for applying supply–demand analysis to experimental systems. A number of examples from the literature are discussed.

5.1. Double modulation

The classical method for performing a supply–demand analysis is based on the double-modulation method of metabolic control analysis, originally introduced by Kacser and Burns (1979). The requirements are that a system can be partitioned around an intermediary metabolite whose concentration can be readily determined, thus separating the pathway into a supply and a demand block. The pathway flux must also be measurable. Independent modulations are then made in the supply and demand blocks (through overexpression of an enzyme, adding an inhibitor, varying the initial pathway substrate concentration, or other means), and the resulting changes in pathway flux and intermediate concentration monitored. The variation of flux with intermediate concentration for the supply perturbation yields the demand rate characteristic, and vice versa.

The double-modulation method forms the basis for the "top-down" (Brown *et al.*, 1990) and "modular" (Schuster *et al.*, 1993) approaches to metabolic control analysis. Importantly, though, in these analyzes, the aim is to obtain elasticities that can be used for the calculation of control coefficients, and consequently only small perturbations around the reference

steady state are required. By contrast, supply–demand analysis aims to paint a picture of the regulation of a system over a wide range (Fig. 25.5). Larger parameter variations are thus considered, but still using the general methodology of double modulation.

In our group, we have applied this method to perform a supply–demand analysis of fermentative anaerobic free-energy metabolism in *Saccharomyces cerevisiae* (Kroukamp *et al.*, 2002). The yeast was grown anaerobically in energy-limited low-glucose chemostat cultures; the demand for cellular free energy (ATP) was perturbed by adding an uncoupler (benzoic acid) at various concentrations, while the supply was perturbed by changing the dilution rate to give different residual glucose concentrations in the chemostat. The measured elasticities ($\varepsilon^{v_{\text{supply}}}_{\text{ATP/ADP}} = -0.84$, $\varepsilon^{v_{\text{demand}}}_{\text{ATP/ADP}} = 7.2$) were used to calculate the control coefficients ($C^{J}_{\text{supply}} = 0.9$, $C^{J}_{\text{demand}} = 0.1$), showing that the bulk of flux control resided in the supply under the conditions used in the investigation (Kroukamp *et al.*, 2002), and that the ATP/ADP concentration ratio was under strong homeostatic control. These results contrasted with those obtained by Schaaff *et al.* (1989), who overexpressed a series of glycolytic enzymes in yeast grown in batch culture, singly and in combination, and found that none of these manipulations affected the glycolytic flux. Possible explanations for the discrepancies between these two studies could be that the latter did not include overexpression of the glucose transporter, or that the different experimental conditions—glucose-limited chemostat versus glucose-excess batch culture—account for the observed differences. At low glucose concentration, the lower activity of the glucose transporter would increase its flux-control coefficient (Kroukamp *et al.*, 2002).

5.2. Selected examples of experimental supply–demand analysis

The first verification of the prediction by Hofmeyr and Cornish-Bowden (2000) that control of flux in many instances lies outside pathways, such as glycolysis, that form part of intermediary metabolism was provided by Koebmann *et al.* (2002) in their study of the control of glycolytic flux in *Escherichia coli* (see Oliver, 2002). They developed a molecular genetic tool that specifically induces ATP hydrolysis in living cells without interfering with other aspects of metabolism, with which they showed that the majority ($>75\%$) of the control of growth rate resides in the demand for ATP, and not in the glycolytic supply. A later study by Causey *et al.* (2003) provided further support for these findings. The results from *E. coli* differ from those of yeast discussed in the previous section, but again it is difficult to compare the results because of differences in the experimental conditions, as the experiments by Koebmann *et al.* (2002) were also performed under glucose excess in batch culture.

Since these studies, a number of experimental investigations into the nature of metabolic regulation in a variety of organisms have explicitly used the supply–demand analytic approach. The study of the control of biosynthetic flux to glycogen in muscle by Schafer *et al.* (2004) is particularly interesting in that here flux control was shown to reside in the supply of glucose-6-phosphate (G6P), specifically in the GLUT4 glucose transporter (not, as previously thought (Roach, 2002), in the demand with glycogen synthase the purported rate-limiting step). They found that G6P homeostasis is achieved by insulin-dependent phosphorylation and allosteric activation of glycogen synthase sensitivity to the upstream G6P. This regulatory mechanism allows muscle cells to tolerate large flux increases across their transporters without significantly changing their own metabolite pools; it is another instance of the functional differentiation predicted by supply–demand analysis: when supply controls the flux, homeostatic maintenance of metabolite concentrations becomes the function of the demand. Supply–demand analysis was therefore instrumental in solving the apparent paradox of glycogen synthase being sensitive to allosteric and covalent regulation despite having a minimal role in flux control.

Mendoza-Cózatl and Moreno-Sánchez (2006) explicitly used supply–demand rate characteristics in their study of the control of glutathione (GSH) and phytochelatin synthetic flux under cadmium stress. Their kinetic model was based on data obtained from GHS synthesis in tobacco cell suspension cultures during illumination. They found that when the GSH supply system was studied in isolation, γ-glutamylcysteine synthetase, which is feedback-inhibited by GSH, is rate limiting. However, in the full supply–demand system that took into account the GSH-consuming reactions, low demand activity exerted most of the flux control, while at high demand, the supply and demand blocks shared the control of flux.

Another instance of flux-control by demand and homeostatic maintenance of concentration by supply was found by Jørgensen *et al.* (2004), who studied the regulatory role of CTP synthase in the biosynthesis of CTP and dCTP in *Lactococcus lactis*. They found that CTP synthase, a supply enzyme, has no control on the growth rate but a strong control on the CTP and dCTP concentrations, as predicted by supply–demand analysis.

These experimental studies are excellent examples of the explanatory power of supply–demand analysis. Space precludes the discussion of other studies, but the reader is encouraged to follow-up Aledo *et al.* (2008), Boada *et al.* (2004), de Atauri *et al.* (2005), McCormick *et al.* (2009), Meléndez-Hevia and Paz-Lugo (2008), Nazaret and Mazat (2008), Santos *et al.* (2006), and Yuan *et al.* (2009). Supply–demand analysis also holds important implications for biotechnology, especially with regard to designing strategies for manipulating the metabolic behavior of organisms (Cornish-Bowden *et al.*, 1995).

ACKNOWLEDGMENT

The authors acknowledge financial support from the South African National Research Foundation (NRF). Any opinion, findings, and conclusions or recommendations expressed in this material are those of the authors, and therefore the NRF does not accept any liability in regard thereto.

REFERENCES

Aledo, J. C., Jiménez-Rivérez, S., Cuesta-Munoz, A., and Romero, J. M. (2008). The role of metabolic memory in the ATP paradox and energy homeostasis. *FEBS J.* **275,** 5332–5342.

Atkinson, D. E. (1977). Cellular Energy Metabolism and Its Regulation. Academic Press, New York.

Boada, J., Cuesta, E., Perales, J. C., Roig, T., and Bermudez, J. (2004). Glutathione content and adaptation to endogenously induced energy depletion in Mv1Lu cells. *Free Radic. Biol. Med.* **36,** 1555–1565.

Brown, G. C., Hafner, R. P., and Brand, M. D. (1990). A 'top-down' approach to the determination of control coefficients in metabolic control theory. *Eur. J. Biochem.* **188,** 321–325.

Causey, T. B., Zhou, S., Shanmugam, K. T., and Ingram, L. O. (2003). Engineering the metabolism of *Escherichia coli* W3110 for the conversion of sugar to redox-neutral and oxidized products: Homoacetate production. *Proc. Natl. Acad. Sci. USA* **100,** 825–832.

Cornish-Bowden, A., Hofmeyr, J.-H. S., and Cárdenas, M. L. (1995). Strategies for manipulating metabolic fluxes in biotechnology. *Bioorg. Chem.* **23,** 439–449.

de Atauri, P., Orrell, D., Ramsey, S., and Bolouri, H. (2005). Is the regulation of galactose 1-phosphate tuned against gene expression noise? *Biochem. J.* **387,** 77–84.

Fell, D. A., and Sauro, H. M. (1985). Metabolic control and its analysis. Additional relationships between elasticities and control coefficients. *Eur. J. Biochem.* **148,** 555–561.

Heinrich, R., and Rapoport, T. A. (1974). A linear steady-state treatment of enzymatic chains: General properties, control and effector strength. *Eur. J. Biochem.* **42,** 89–95.

Hofmeyr, J.-H. S. (1995). Metabolic regulation: A control analytic perspective. *J. Bioenerg. Biomembr.* **27,** 479–490.

Hofmeyr, J.-H. S. (1997). Anaerobic energy metabolism in yeast as a supply-demand system. *In* "New Beer in an Old Bottle: Eduard Buchner and the Growth of Biochemical Knowledge," (A. Cornish-Bowden, ed.), pp. 225–242. Universitat de València, València, Col.lecció Oberta.

Hofmeyr, J.-H. S. (2008). The harmony of the cell: The regulatory design of cellular processes. *Essays Biochem.* **45,** 57–66.

Hofmeyr, J.-H. S., and Cornish-Bowden, A. (1991). Quantitative assessment of regulation in metabolic systems. *Eur. J. Biochem.* **200,** 223–236.

Hofmeyr, J.-H. S., and Cornish-Bowden, A. (1996). Co-response analysis: A new experimental strategy for metabolic control analysis. *J. Theor. Biol.* **182,** 371–380.

Hofmeyr, J.-H. S., and Cornish-Bowden, A. (1997). The reversible Hill equation: How to incorporate cooperative enzymes into metabolic models. *Comput. Appl. Biosci.* **13,** 377–385.

Hofmeyr, J.-H. S., and Cornish-Bowden, A. (2000). Regulating the cellular economy of supply and demand. *FEBS Lett.* **476,** 47–51.

Hofmeyr, J.-H. S., Kacser, H., and van der Merwe, K. J. (1986). Metabolic control analysis of moiety-conserved cycles. *Eur. J. Biochem.* **155,** 631–641.

Hofmeyr, J.-H. S., Cornish-Bowden, A., and Rohwer, J. M. (1993). Taking enzyme kinetics out of control; putting control into regulation. *Eur. J. Biochem.* **212,** 833–837.

Jørgensen, C. M., Hammer, K., Jensen, P. R., and Martinussen, J. (2004). Expression of the pyrG gene determines the pool sizes of CTP and dCTP in *Lactococcus lactis*. *Eur. J. Biochem.* **271,** 2438–2445.

Kacser, H., and Burns, J. A. (1979). Molecular democracy: Who shares the controls? *Biochem. Soc. Trans.* **7,** 1149–1160.

Kacser, H., Burns, J. A., and Fell, D. A. (1995). The control of flux: 21 years on. *Biochem. Soc. Trans.* **23,** 341–366.

Koebmann, B. J., Westerhoff, H. V., Snoep, J. L., Solem, C., Pedersen, M. B., Nilsson, D., Michelsen, O., and Jensen, P. R. (2002). The extent to which ATP demand controls the glycolytic flux depends strongly on the organism and conditions for growth. *Mol. Biol. Rep.* **29,** 41–45.

Kroukamp, O., Rohwer, J. M., Hofmeyr, J.-H. S., and Snoep, J. L. (2002). Experimental supply-demand analysis of anaerobic yeast energy metabolism. *Mol. Biol. Rep.* **29,** 203–209.

le Novère, N., Bornstein, B., Broicher, A., Courtot, M., Donizelli, M., Dharuri, H., Li, L., Sauro, H., Schilstra, M., Shapiro, B., Snoep, J. L., and Hucka, M. (2006). BioModels Database: A free, centralized database of curated, published, quantitative kinetic models of biochemical and cellular systems. *Nucleic Acids Res.* **34,** D689–D691.

McCormick, A. J., Watt, D. A., and Cramer, M. D. (2009). Supply and demand: Sink regulation of sugar accumulation in sugarcane. *J. Exp. Bot.* **60,** 357–364.

Meléndez-Hevia, E., and Paz-Lugo, P. D. (2008). Branch-point stoichiometry can generate weak links in metabolism: The case of glycine biosynthesis. *J. Biosci.* **33,** 771–780.

Mendoza-Cózatl, D. G., and Moreno-Sánchez, R. (2006). Control of glutathione and phytochelatin synthesis under cadmium stress. Pathway modeling for plants. *J. Theor. Biol.* **238,** 919–936.

Nazaret, C., and Mazat, J.-P. (2008). An old paper revisited: "A mathematical model of carbohydrate energy metabolism. interaction between glycolysis, the Krebs cycle and the H-transporting shuttles at varying ATPases load" by V. V. Dynnik, R. Heinrich and E.E. Sel'kov. *J. Theor. Biol.* **252,** 520–529.

Oliver, S. (2002). Metabolism: Demand management in cells. *Nature* **418,** 33–34.

Olivier, B. G., and Snoep, J. L. (2004). Web-based kinetic modelling using JWS Online. *Bioinformatics* **20,** 2143–2144.

Olivier, B. G., Rohwer, J. M., and Hofmeyr, J.-H. S. (2005). Modelling cellular systems with PySCeS. *Bioinformatics* **21,** 560–561.

Reich, J. G., and Sel'kov, E. E. (1981). Energy metabolism of the cell: A theoretical treatise. Vol. 29 of Koebmann *et al.* (2002).

Roach, P. J. (2002). Glycogen and its metabolism. *Curr. Mol. Med.* **2,** 101–120.

Rohwer, J. M., and Hofmeyr, J.-H. S. (2008). Identifying and characterising regulatory metabolites with generalised supply-demand analysis. *J. Theor. Biol.* **252,** 546–554.

Rohwer, J. M., and Hofmeyr, J.-H. S. (2010). Kinetic and thermodynamic aspects of enzyme control and regulation. *J. Phys. Chem.B* **114,** 16280–16289.

Santos, V., Galdeano, C., Gomez, E., Alcon, A., and Garcia-Ochoa, F. (2006). Oxygen uptake rate measurements both by the dynamic method and during the process growth of *Rhodococcus erythropolis* IGTS8: Modelling and difference in results. *Biochem. Eng. J.* **32,** 198–204.

Schaaff, I., Heinisch, J., and Zimmermann, F. K. (1989). Overproduction of glycolytic enzymes in yeast. *Yeast* **5,** 285–290.

Schafer, J. R. A., Fell, D. A., Rothman, D., and Shulman, R. G. (2004). Protein phosphorylation can regulate metabolite concentrations rather than control flux: The example of glycogen synthase. *Proc. Natl. Acad. Sci. USA* **101,** 1485–1490.

Schuster, S., Kahn, D., and Westerhoff, H. V. (1993). Modular analysis of the control of complex metabolic pathways. *Biophys. Chem.* **48,** 1–17.

Smallbone, K., Simeonidis, E., Swainston, N., and Mendes, P. (2010). Towards a genome-scale kinetic model of cellular metabolism. *BMC Syst. Biol.* **4,** 6.

Yuan, J., Doucette, C. D., Fowler, W. U., Feng, X.-J., Piazza, M., Rabitz, H. A., Wingreen, N. S., and Rabinowitz, J. D. (2009). Metabolomics-driven quantitative analysis of ammonia assimilation in *E. coli*. *Mol. Syst. Biol.* **5,** 302.